Talanta 305 (2026) 129575

Contents lists available at ScienceDirect

Talanta

journal homepage: www.elsevier.com/locate/talanta

# Towards the harmonization of raw data processing in single particle inductively coupled plasma mass spectrometry

Isabel Abad-Alvaro, Eduardo Bolea, Francisco Laborda *

*Group of Analytical Spectroscopy and Sensors (GEAS), Institute of Environmental Sciences (IUCA), University of Zaragoza, Pedro Cerbuna 12, 50009, Zaragoza, Spain*

ARTICLE INFO

*Keywords:*
Single particle analysis
SP-ICP-MS
Data processing
Harmonization
Validation

ABSTRACT

Despite the availability of advanced data processing tools for single particle inductively coupled plasma mass spectrometry (SP-ICP-MS), users cannot fully trust on them to obtain reliable and accurate information due to their lack of validation. Along this work, current approaches for data processing have been evaluated in depth, paying special attention to the criteria and expressions used for calculation of critical values concerning the discrimination of baseline and particle readings, the counting of particle events and the determination of their total intensities, in order to promote their harmonization within the field, although focusing on quadrupole instruments. Baseline intensity was the most critical variable, since its magnitude determines which approach, Poisson or Gaussian, must be applied for discrimination of baseline and particle readings depending on its magnitude. Application of the corresponding approaches with a coverage factor of 5 led to the occurrence of less than 10 false positives (baseline readings considered as particle events) in a variety of experimental conditions (baseline intensities, number of readings, dwell times). The use of less demanding coverage factors (e.g., 3) led to increased false positives, particularly in the presence of nano- and microparticles and working at short dwell times, due to the higher occurrence of low-intensity particle events. Therefore, such conditions should be avoided.

Processing data from nano and microparticle suspensions measured at different dwell times and baseline levels with the free-access and open-source tool SPCal, resulted in reliable counting numbers and total intensities when the adequate critical values were applied. Consequently, this tool allowed the validation of a proprietary software as a proof of concept, confirming comparable results, except for the counting of particle events with high baseline levels or when using short dwell times, as long as the proposed approaches for the calculation of critical values, which were not originally implemented in such proprietary software, were applied.

## 1. Introduction

After ten years from the launching of the first commercial inductively coupled plasma mass spectrometer with single particle detection capability [1] and more than twenty years of the conception of single particle inductively coupled plasma mass spectrometry (SP-ICP-MS) [2], the technique has already experienced a period of intense activity focused on achieving a broad view of the technique at instrumental, metrological and methodological levels. As a result, SP-ICP-MS methods are now applied to a wide range of analytical problems and the technique has become established as a routine tool with wide commercialization [3–5]. According to Horlick [6], it can be said that SP-ICP-MS has passed its characterization stage and it can be considered mature. However, a number of issues related to the metrological aspects of the technique, as well as to data processing, still require a higher level of harmonization to expand and facilitate a solid implementation of SP-ICP-MS.

The growth of SP-ICP-MS was related to the commercialization of fast data acquisition ICP-MS spectrometers, which allowed the use of dwell times down to 10 μs instead of working in the millisecond range [1,7]. Since the duration of the particle events is in the range of several hundreds of microseconds, using millisecond dwell times makes that events are recorded as pulses (1-reading events), whereas they are recorded as peaks when using microsecond dwell times, consisting of several readings. Thus, data processing, that could be performed by using spreadsheets (e.g., Single Particle Calculation (SPC) tool [8]) when 1-reading events are obtained, required the use of more

This article is part of a special issue entitled: SC/SP approaches for ICP-MS published in Talanta.

* Corresponding author.
*E-mail address:* flaborda@unizar.es (F. Laborda).

https://doi.org/10.1016/j.talanta.2026.129575
Received 12 September 2025; Received in revised form 23 January 2026; Accepted 20 February 2026
Available online 20 February 2026
0039-9140/© 2026 The Authors. Published by Elsevier B.V. This is an open access article under the CC BY-NC-ND license (http://creativecommons.org/licenses/by-nc-nd/4.0/).

sophisticated tools. This led to the development of new programs for data processing that ICP-MS manufacturers incorporated as specific modules in their software [7]. The disadvantages of such proprietary software are that the algorithms implemented are not always available and their validation is not straightforward. The different data processing tools used in SP-ICP-MS have recently been summarized and reviewed by Chronakis et al. [9]. In this regard, open-source and free-access software have become available for SP-ICP-MS data processing (SPCal [10,11] at https://github.com/djdt/spcal and TOF-SPI [12] at https://github.com/TOFMS-GG-Group/TOF-SPI). In the case of TOF-SPI, it is a software for processing data from a specific ICP-TOF instrument written in LabVIEW, whereas SPCal is an open-source software that accepts raw data from any type of ICP-MS spectrometer, also including mass scans recorded with ICP-TOF-MS instruments.

Metrological harmonization involves clear criteria for data processing and procedures for determination of the different measurands available in SP-ICP-MS, as well as expressions for estimation of the corresponding detection limits. Recently, ISO has revised a previous version of a technical specification on SP-ICP-MS published in 2019 [13], covering aspects related to calibrations and experimental procedures but not basic processing of raw data. Regarding detection limits, the approaches developed by Currie for the estimation of concentration detection limits for Poisson distributed data [14] were adapted to SP-ICP-MS, and criteria and expressions for element mass per particle, particle size and number concentration detection limits have been proposed [15,16].

The critical step of data processing in SP-ICP-MS involves the discrimination of readings from the baseline and those corresponding to the particle events. The most frequently applied approach is based on the application of a threshold value defined from the standard deviation of the baseline ($z$-sigma criteria), where particle readings exceeding the threshold are considered as outliers [17,18]. The simplest way of applying such approach to a dataset is averaging the entire dataset, removing all readings that are above their mean plus a defined multiple $n$ of their standard deviation, and reprocessing iteratively the remaining readings until there are no more readings to remove [17]. This approach assumes that the baseline follows a Gaussian distribution. However, ICP-MS signals are governed by Poisson processes [19], which only lead to Gaussian distributions at high-count intensities, when flicker noise predominates; otherwise, shot noise prevails, which follows Poisson-like distributions. Laborda et al. [15] considered the Poisson nature of low-count baselines when working with quadrupole instruments due to the counting statistics of the electron multiplier detectors, while Gundlach-Graham et al. [20] proved that in modern time-of-flight instruments baselines follow compound Poisson distributions, which present an additional noise component due to the gain statistics of the fast analog-to-digital conversion of the microchannel-plate detector currents. In both cases, baseline standard deviations are not measured directly but estimated as the squared root of the baseline count-intensity [14]. In the case of quadrupole instruments, the particular behavior of the baseline has led to the application of the so-called Poisson and Gaussian filters depending on the baseline intensity when processing data sets [10].

The consideration of the SP-ICP-MS baseline readings and the resulting distribution as a blank measurement allows to adapt the concept of critical value, developed by Currie to describe the detection capability of a conventional quantitative method [14], and to handle the threshold as a critical value [15,20]. A conventional critical value is defined as the response of the instrument above which an observed signal is reliably attributed to the presence of analyte, implying that there is a certain probability that it is falsely detected, producing a false positive. In SP-ICP-MS the critical value allows the control of the number of false positives (baseline readings considered as particle readings), which should be zero [21] or kept to a minimum [22], to avoid degradation of the number concentration detection limits. Such zero-level of false positives can be achieved since baseline distributions in SP-ICP-MS are not continuous but discrete, and can be controlled by the $z$ factor discussed above. Despite a factor of 3 is widely applied [17], adopting the typical value involved in conventional expressions used for calculation of concentration detection limits, removal of false positives is incomplete and the use of a factors of 5 has been demonstrated to be a fair compromise between avoiding false positives without degrading the detectability of small particles under different data acquisition conditions [16,21,23].

Despite all the advances on data processing and their implementation in different tools, such as those described above, SP-ICP-MS users still seem to be unaware of its relevance or remain reluctant to harmonize data processing. For illustrative purposes, only half of the 88 articles published in 2024 on quadrupole SP-ICP-MS reported the software/tool used for data processing. Among those who reported it, half of the works used the software provided by the manufacturers of the instruments, whereas 25% used in-house developed tools (spreadsheets or programs written in Phyton, MATLAB, GNU Octave, R). In the other 25%, free-access tools (SPC spreadsheet or SPCal, mainly) or a software formerly developed for laser ablation ICP-MS (Hyper Dimensional Image Processing software) were used. Regarding the thresholding criteria applied, they were only reported in one third of the papers, with 3-sigma being the most commonly used (43%), closely followed by 5-sigma (36%). However, more than 20% reported the use of other alternative criteria. In any case, a Gaussian behavior of the baseline was considered in most of the works and less than 7% of the total publications considered the Poisson behavior.

Considering the current availability of free-access, open-source and well-documented tools for data processing, SP-ICP-MS users have the opportunity to check and validate their results, as well as the tools they are using, in a more flexible way. However, the use of such tools requires an adequate knowledge of the criteria and procedures to be applied. Hence, the objectives of this work are the evaluation of the different criteria and expression available for calculation of critical values in SP-ICP-MS under a variety of experimental conditions by using the free-access software SPCal, the validation of this tools and the comparison of the attainable results by using a proprietary software. The ultimate aim is to establish robust criteria that can contribute to the harmonization of data processing and the validation of data processing tools in SP-ICP-MS.

## 2. Experimental

### 2.1. Instrumentation

A PerkinElmer NexION 2000B mass spectrometer (Toronto, Canada) was used for ICP-MS measurements in single particle mode. The sample introduction system consisted of a glass concentric nebulizer and a baffled cyclonic spray chamber (Meinhard) for the introduction of nanoparticles. In this case, argon nebulizer gas flow of 1.02 L $min^{-1}$ and sample flow rate of 0.377 mL $min^{-1}$ were used. For the analysis of microparticles, an Asperon™ linear pass spray chamber sample introduction system (PerkinElmer, Toronto, Canada), equipped with a flow focusing nebulizer (Ingeniatrics, Sevilla, Spain) was used. In this case, a μDx Single Cell Autosampler (Elemental Scientific, Omaha, NE, USA) equipped with a syringe pump operating at 10 μL $min^{-1}$ was used for sample introduction. Argon nebulizer and make-up gas flows were 1 L $min^{-1}$ and 0.2 L $min^{-1}$, respectively.

### 2.2. Standards

Diluted suspensions of gold nanoparticles (AuNPs), silver nanoparticles (AgNPs) and polystyrene (PS) microparticles were prepared from commercially available suspensions. Monodisperse citrate-stabilized gold nanoparticles of nominal diameter 51 nm were obtained from nanoComposix (San Diego, CA, USA). LGCQC5050 citrate-stabilized gold nanoparticles of nominal diameter 30 nm was obtained

from LGC Limited (Teddington, UK). Silver nanoparticles with a nominal diameter of 75 nm was obtained from NIST (NIST, Gaithersburg, USA – RM 8017 polyvinylpyrrolidone coated). Polystyrene microparticles suspensions with diameter 3.03 ± 0.09 μm were purchased from Sigma (Sigma Aldrich, Switzerland). Reference latex sphere suspensions of 2.223 ± 0.013 μm diameter (RM165) were obtained from BCR (Geel, Belgium).

Aqueous gold and silver solutions were prepared from standard stock solutions of 1000 mg $L^{-1}$ (Sigma Aldrich, Switzerland) by dilution in ultrapure water.

### 2.3. Procedures

*Standard suspensions.* Dilutions of the stock suspension of gold and silver nanoparticles and polystyrene microparticles were prepared in ultrapure water (Milli-Q Advantage, Molsheim, France) by accurately weighing (±0.1 mg) aliquots after 1 min sonication. After dilution and before each analysis, the suspensions were bath sonicated for 1 min.

*SP-ICP-MS measurements.* Suspensions were measured in single particle mode using the Syngistix Nano-Application module version 3.2 (PerkinElmer Inc.) The dwell times used were in the range of 5 ms to 25 μs with total acquisition times of 60 s, recording from 12,000 (at 5 ms) up to 2,400,000 (at 25 μs) readings per time scan, respectively. Sample flow rate was measured daily gravimetrically.

*Data processing.* Recorded time scan files were exported and processed with the SPCal software version 1.3.3 [24] using iterative thresholding and the Poisson or the Gaussian filter option, depending on the baseline intensity. The scans were also processed by using the software provided by the manufacturer (Syngistix Nano-Application module version 3.2) by applying selected thresholds in manual mode or the 5-sigma threshold available in automatic mode.

## 3. Results and discussion

### 3.1. Discrimination of baseline/particle readings: calculation of the critical value

Although a number of criteria have been adopted to discriminating particle readings from those of the baseline, there is a consensus to adopt very restrictive criteria to eliminate as far as possible all baseline readings and thus minimize the occurrence of false positives, which would be considered as particles and would degrade the number concentration detection limits [21,22]. On the other hand, the application of too restrictive criteria can affect negatively the size/mass of elements per particle detection limits and should be avoided. The threshold for such discrimination is estimated as a critical value ($Y_C$), which is typically expressed as:

$$Y_C = Y_B + z_{1-\alpha}\sigma_B \quad (1)$$

where $Y_B$ is the mean baseline intensity, $z_{1-\alpha}$ denotes the $(1-\alpha)$ quantile of the standard normal distribution, $\alpha$ is the probability of false positives for a standard normal distribution and $\sigma_B$ the standard deviation of the baseline.

The estimation of $\sigma_B$ deserves special attention since it depends on the noise behavior of the instrument, as discussed in the Introduction. Quadrupole and double focusing instruments, equipped with electron multipliers, show a Poisson-distributed noise for low-count readings, whereas for high-count readings, flicker noise (ξ) becomes more significant and the baseline distributions tend to Gaussian profiles. For baselines over 10 counts, noise cannot be described solely by Poisson statistics and $\sigma_B$ can be calculated directly from the standard deviation of the baseline readings (Gaussian filter). Application of Poisson statistics to baselines below 10 counts (Poisson filter) involves estimating $\sigma_B$ from the square root of the baseline intensity. Although for Poisson distributed data $\sigma_B = \sqrt{Y_B}$, Currie proposed the following expression when handling low signals (below 5 counts) [25]:

$$Y_C = Y_B + z_{1-\alpha}\sqrt{Y_B + \varepsilon} \quad (2)$$

where $\varepsilon$ is a correction factor for estimation of the baseline variance, that can range from 0 to 1 [25]. As discussed in the Supplementary Information, the inclusion of a $\sqrt{\eta}$ factor ($\eta = 2$ for paired measurements) in the last term of the expression is not justified since $Y_C$ is not handled as a net critical value.

Alternatively, expressions other than equation (2) have been proposed in the context of radiometric measurements and radiation counting. They are summarized in the MARLAP document *Detection and Quantification Capabilities* [26], that have been considered in several SP-ICP-MS publications [11,15]. All these expressions have been critically evaluated in this work (Table SI1 and Figure SI1), concluding that their use is not justified in the context of SP-ICP-MS, as discussed in the Supplementary Information.

In this context, the quantile $z_{1-\alpha}$ (or $\alpha$) must be selected to avoid the occurrence of false positives arising from the baseline, as discussed above, and it must be considered as a coverage factor instead of a conventional $z$-score. Mehrabi et al. [27] reported a dynamic alpha approach to control the fraction of false positives from the baseline in SP-ICP-TOF-MS, while setting the critical value as low as possible to record low-intensity particle events. Alpha was selected for each isotope according to a user-defined ratio of detected particle events:predicted false positive events (typically 1000:1) and implemented in the workflow of the data processing software [12]. Laborda et al. [16,21] proposed the use of a $z_{1-\alpha} = 5$ ($\alpha = 2.87\text{x}10^{-7}$) to guarantee the absence of false positives in a wide range of experimental conditions (baseline intensities, number of readings, dwell times, total acquisition times) on empirical basis.

#### 3.1.1. Basic evaluation considering blank baselines

As a first approach, the in-depth evaluation of equation (2) for calculation of critical values was based on theoretical and experimental baselines produced in the absence of particles.

The number of false positives for baseline intensities in the range of 0.1-10 counts was estimated from the corresponding theoretical discrete Poisson distribution after applying the critical value calculated from equation (2) ($z_{1-\alpha} = 5$) for different $\varepsilon$ values (Figure SI2). Although 10 false positives or less could be obtained for baseline intensities from 1 to 10 counts with no application of this correction factor, false positives could be reduced to 5 or less by applying $\varepsilon = 0.5$ and to 1-2 by for $\varepsilon = 1$. For baseline intensities below 1 count, such correction factor must be applied ($\varepsilon = 0.5$-1) to guarantee a low level of false positives. The choice of 0.5 or 1 leads to increase the critical values from 0 to 2 counts, depending on the baseline intensity, which does not increase severely size detection limits. Hence, expecting higher occurrence of false positives with experimental measurements in the range of baseline intensities up to 10 counts, application of equation (2) with $\varepsilon = 1$ is recommended.

Fig. 1 shows theoretical baseline intensity distributions, calculated as described in the Supplementary Information, and experimental ones obtained by measuring solutions of Ag(I) of different concentrations. For baseline intensities of 10 counts or lower, critical values were calculated from equation (2) ($z_{1-\alpha} = 5$, $\varepsilon = 1$), whereas for baselines higher than 10 counts equation (1) ($z_{1-\alpha} = 5$; $\sigma_B = \sqrt{Y_B + \xi^2 Y_B^2}$ (equation SI.3); $\xi = 0.1$) was applied. Fair agreement between theoretical and experimental distributions was obtained, what confirms the Poisson and Gaussian behavior of the baselines when measured with electron multiplier detectors. On the other hand, the expressions and parameters selected allowed to minimize the occurrence of false positives.

Fig. 2 summarizes the experimental occurrence of false positives after calculating critical values according to the baseline mean intensity. Baselines of different mean intensities were obtained by measuring

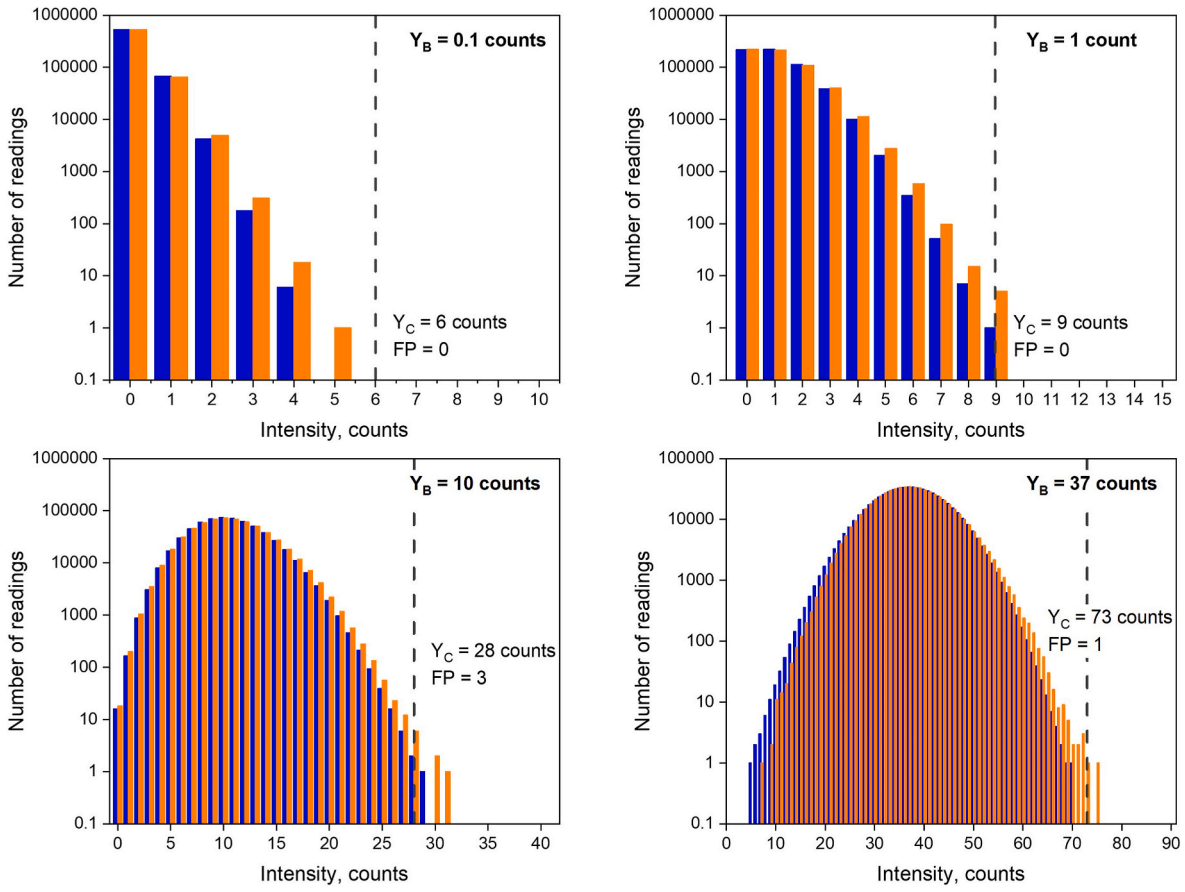


**Fig. 1.** Comparison of theoretical (blue) and experimental (orange) baseline intensity distributions (0.1, 1, 10 and 37 counts) and occurrence of false positives (FP) after calculating critical values with equation (1) ($Y_B$ >10 counts) and 2 ($Y_B$ ≤10 counts), $z_{1-\alpha} = 5$, $\varepsilon = 1$. Experimental distributions obtained by measuring Ag(I) solutions of different concentrations. Dwell time: 100 μs. Acquisition time: 60 s. Number of readings: 6x10$^5$.

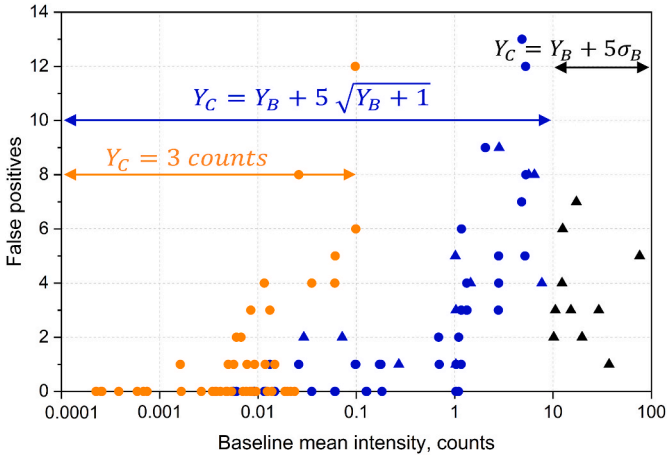


**Fig. 2.** Experimental number of false positives (FP) after calculating critical values according to the baseline mean intensity: $Y_B > 10$ counts, $Y_C = Y_B + 5\sigma_B$ (black triangles); $1 \leq Y_B \leq 10$ counts, $Y_C = Y_B + 5\sqrt{Y_B + 1}$ (blue); $Y_B$ <0.1 counts, $Y_C$ = 3 counts (orange). Dwell time: 100 μs. Acquisition time: 60 s. Number of readings: 6x10$^5$. Dots: individual measurements of different isotopes in ultrapure water. Triangles: Ag(I) solutions of different concentrations.

ultrapure water (dwell time: 100 μs, acquisition time 60 s) monitoring different isotopes, as well as Ag(I) solutions of different concentrations. For baseline mean intensities over 10 counts, application of equation (1) (Gauss filter) considering $z_{1-\alpha} = 5$ allowed to obtain less than 10 false positives under the conditions studied. Application of the Currie expression (equation (2)) with $z_{1-\alpha} = 5$ and $\varepsilon = 1$ allowed to obtain less than ca. 10 false positives for baselines below 10 counts, although 0-2 false positives were usually measured for baselines below 1 count. However, for baselines lower than ca. 0.1 counts, the application of the selected criterion provided critical values too high ($Y_C = 6$ counts) for fully removing of false positives. Since theoretical baselines below 0.01 counts mainly consist of 0 count readings and a smaller proportion of 1 and 2 counts readings, a critical value of 3 counts could be a fair compromise to avoid false positives while keeping low detection limits. Blank baselines measured for different isotopes (dwell time: 100 μs, total acquisition time: 60 s, number of readings: 6x10$^5$) are summarized in Table SI2, confirming this approach, that can be extended up close to 0.1 counts assuming an occurrence of less than 5 false positives. For extremely low intensities below 0.001 counts the critical values could even be reduced to 2 counts with no adverse effect on the occurrence of false negatives.

Hence, the broadly accepted approach of applying a threshold criterion based on the standard deviation of the baseline (equation (1)) is valid for baseline mean intensities over 10 counts, whereas for lower intensities the Currie expression (equation (2)) should be used. The use of these equation with $z_{1-\alpha} = 5$ and $\varepsilon = 1$ guarantees false positive occurrence below ca. 10. However, for intensities below 1 count the proposed Currie expression overestimates critical values, degrading attainable size detection limits, so it might be exchanged by applying a critical value of 3 counts, or even 2 counts for baselines below 0.001 counts. These recommendations are based on experimental measurements consisting of 6x10$^5$ readings, for measurements with more or less readings the approach is still valid, as it can be seen in Table 1 for the analysis of a 0.1 μg L$^{-1}$ Ag(I) solution producing a count rate signal of

**Table 1**
Effect of the number of readings and the baseline mean intensity at different dwell times on the occurrence of false positives. Ag(I) 0.1 μg $L^{-1}$. Acquisition time: 60 s n = 3.

| dwell time μs | number of readings | $Y_B$[a] counts | $Y_C$[b] counts | false positives[c] |
|---|---|---|---|---|
| 50 | $1.2x10^6$ | 0.1296 | 6 | 1 |
| 100 | $6.0x10^5$ | 0.2726 | 6 | 1 |
| 200 | $3.0x10^5$ | 0.5570 | 7 | 2 |
| 500 | $1.2x10^5$ | 1.4030 | 10 | 1 |
| 1000 | $6.0x10^4$ | 2.7657 | 13 | 0 |
| 5000 | $1.2x10^4$ | 13.5967 | 33 | 1 |

[a] mean intensity (n = 3).
[b] equation (1) ($Y_B$ >10 counts) and 2 ($Y_B$ ≤10 counts).
[c] median (n = 3).

2.8 cps measured at different dwell times in single particle mode.

### 3.1.2. *Effect of nanoparticles on baselines*

Whereas the presence of nanoparticles below the critical value (in size) will contribute to the mean intensity of the baseline, modifying the expected model distributions discussed above [28], larger particles should not affect the baseline unless dissolved forms of the element are present in the suspension, which would increase the mean baseline intensity while maintaining the distribution profile.

Fig. 3a and 3b shows the intensity distributions of 50 nm AuNPs measured at dwell times of 100 and 25 μs. Nanoparticle size was selected to yield a distribution clearly separated from that of the baseline. Raw data were processed applying equation (2) ($z_{1-\alpha}$ = 5 and $\varepsilon$ = 1) and critical values of 6 counts were obtained in both cases. A critical value of 3 counts was also checked since it has been suggested as a fair alternative for improving detectability in the previous section. The contribution of the nanoparticles to the baseline can be clearly seen in the distribution obtained at 25 μs dwell time and processed with $Y_C$ = 3 counts (Fig. 3b orange line), where the tail of the baseline distribution was still visible up to 20-25 counts, when the theoretical distribution for the mean baseline intensity measured ended at 2 counts. Application of $Y_C$ = 6 counts (Fig. 3b blue line) allowed to avoid that tail, although a number of particle events up to 80-90 counts were detected in both cases. When using a dwell time of 100 μs both the occurrence of low intensity events and the tail of the baseline counts were avoided (residual false positives were detected for $Y_C$ = 3 counts). Due to the low baseline intensity, application of both critical values at 100 μs dwell time produced the same profile for the intensity distribution of the nanoparticle (only blue line visible in Fig. 3a).

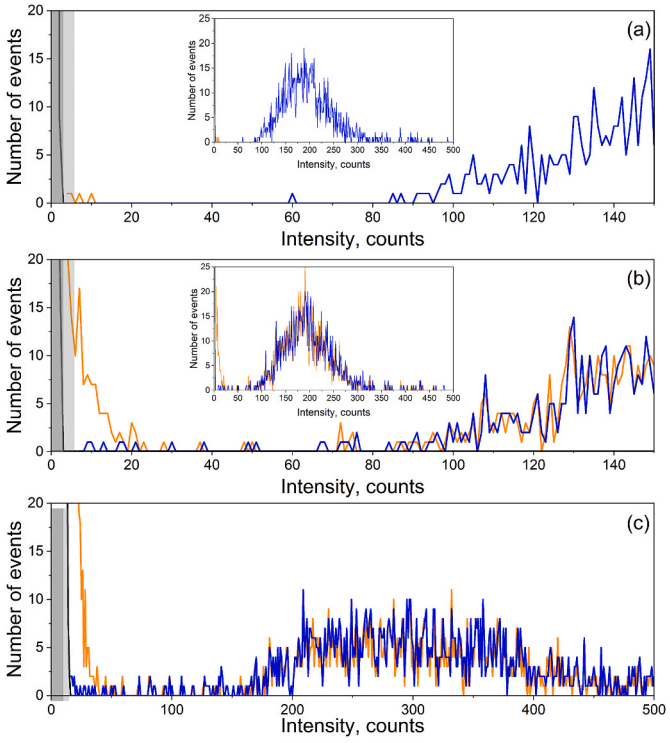


**Fig. 3.** Intensity distributions of 50 nm AuNPs measured at (a) 100 and (b) 25 μs dwell times. Raw data processed considering $Y_C$ = 6 counts (blue) and $Y_C$ = 3 counts (orange; same profile in (a), only blue line shown). Regions corresponding to $Y_C$ ≤6 counts and $Y_C$ ≤3 counts in light and dark grey, respectively. Theoretical baseline distribution in black. $Y_B$ = 0.006 counts (100 μs) and 0.004 counts (25 μs). (c) Intensity distributions of 3 μm polystyrene microparticles measured at 100 μs dwell times. Raw data processed considering equation (2) with $z_{1-\alpha}$ = 5 (orange) and $z_{1-\alpha}$ = 3 (blue). Regions corresponding to $Y_C$ ≤15 counts and $Y_C$ ≤10 counts in light and dark grey. Theoretical baseline distribution in black. $Y_B$ = 3.47 counts.

Fig. 3 c shows the intensity distributions of 3 μm polystyrene microparticles measured at 100 μs dwell time. Polystyrene microparticles produce much broader distributions in comparison with nanoparticles [29], leading to a high proportion of low intensity events. In addition, baseline levels of several counts are typically measured due to the carbon content in water and the presence of residual organic surfactants. Whereas the application of the recommended threshold criterion ($z_{1-\alpha}$ = 5 with and $\varepsilon$ = 1) allowed to avoid the occurrence of false positives from the baseline, the application of a less restrictive criterion ($z_{1-\alpha}$ = 3) did not allow to remove completely the baseline distribution, which showed a relevant tail in comparison with the theoretical distribution. On the other hand, low intensity particle events between the baseline and the microparticle distributions were observed in any case.

Fig. 3 confirms that the particles affect the expected baseline distributions, in connection with data acquisitions conditions and data processing, by producing low intensity events that are incorporated to the baseline readings, increasing the mean intensity of the baseline and modifying its profile, specially at the tail of the distributions. These effects are more evident at shorter dwell times, since particle events are smaller, the intensity of the particle readings is lower and the proportion of readings in the baseline range is higher. A similar effect was observed for highly polydisperse signal distributions, as those obtained with microparticles. Hence, the application of equation (2) with $z_{1-\alpha}$ = 5 and $\varepsilon$ = 1 is highly recommended. For low baseline intensities (<0.1 counts), the minimum critical value of 6 counts obtained from this equation is also the best option to avoid the occurrence of false positives produced by particle artifacts. In relation to avoiding particle artifacts over the critical value (particle events at intensities below the particle distributions), apart from using the appropriate critical value, long dwell times (over ca.100 μs) should be used, although their occurrence is favored in the case of microparticles.

For higher baselines and/or smaller nanoparticles the overlap of both distributions makes the conclusions drawn above less relevant, since only semi-quantitative information on nanoparticles could be obtained [29]. However, for the sake of harmonization, the same discrimination criterion should be maintained.

### 3.2. *Processing of particle events: validation of data processing tools*

Once the critical values have been calculated using the adequate expressions with the appropriate parameter values, the readings that do not correspond to the baseline must be processed to identify the recorded particulate events, count them and obtain their total intensities. Data recorded at dwell times in the millisecond range can be processed by considering each reading as a particle event (e.g., by using a spreadsheet). However, for dwell times below 3 ms the occurrence of split events (particle events recorded in two consecutive readings) increases and detection of such split events must be implemented to avoid overestimating the number of particles counted. Assuming the high

probability of two consecutive readings belong to the same particle event, such readings can be merged as a single event once detected [30]. This inconvenience is overcome when using tools that process particle events as peaks (n-reading events) since split events are 2-reading events in fact. However, identification of peaks as particle events can become problematic with these tools for low intensity events. A number of strategies have been proposed, that include chromatographic approaches based on the searching of inflexion points around a peak maximum of a certain width [7] or the identification of the beginning and end of the events in different ways [31–33]. In any case, once the particle events have been identified they are counted to relate such counting with the number concentration of the particles, whereas the net readings (raw reading intensity minus the mean baseline intensity) corresponding to each event summed up to obtain its total intensity that will be related to the mass of element per particle and to the size of the particles if their shape, composition and density are known or assumed. By summing up the net readings corresponding to each particle, a signal (total intensity) independent of the dwell time used should be obtained.

Identification of peaks as individual particle events can be hindered by the dwell time applied, the size of the particles, the width of the events or the number of readings along the peak, making difficult a systematic evaluation of the different strategies reported in the literature. As an alternative, the data processing software SPCal (version 1.3.3) was evaluated and validated internally with respect to the counting of the number of events and the determination of their mean total intensity. Internal validation consisted in the measurement of a Au nanoparticle suspension at different dwell times under the assumption that both the counting of particle events and their mean total intensity is independent of the dwell time. In a next step, the effect of the baseline intensity level on both parameters was studied by measuring suspensions of Ag nanoparticles in the presence of different concentrations of dissolved silver (I), which again should not affect the counting of particle events and their mean total intensities.

In SPCal, a user-defined number of consecutive readings over the detection threshold are identified as an individual particle event, whose total intensity is the sum of the net readings over a so-called accumulation threshold, which can be selected among the detection threshold, half the detection threshold and the mean intensity of the dataset (a value between the mean baseline intensity and half the detection threshold). The number of readings used to identify particle event was limited to 1, due to the range of dwell times evaluated, particularly the inclusion of millisecond dwell times, where events are predominantly recorded as 1-reading events. Because SPCal calculates the net intensities by subtracting the selected accumulation threshold, the mean intensity option was selected since it was the closest value to the mean baseline intensity.

Fig. 4 shows the result obtained from a suspension of 30 nm Au nanoparticles and concentration $2.8x10^7$ $L^{-1}$ to minimize the occurrence of 2-particle events at long dwell times, measured at dwell times from 50 μs up to 5 ms. Fig. 4a confirms that mean number of events obtained at different dwell times and processed with SPCal were within the 2-sigma interval calculated with the individual values (403 ± 30 events), as it was the case for the mean total intensities (55 ± 4 counts), as it can be seen in Fig. 4b. Regarding the total intensity of particle events, total intensities were slightly higher at the longest dwell times mostly probably due to the occurrence of 2-particle events.

Fig. 5 shows the effect of high baseline levels on the processing of particle events. Suspensions of 75 nm silver nanoparticles were analyzed in the presence of increasing baseline levels by adding dissolved silver. Measurements were performed at 100 μs dwell time. By adding 1.5 and 7 μg $L^{-1}$ of Ag(I), baseline intensities increased from 0.03 counts to 2 and 13 counts, respectively, without affecting the detection of the distribution of silver nanoparticles (figure SI3), but requiring to apply different threshold equations according to the intensity. Fig. 5a confirms that the number of events did not show significant statistical differences when processed with SPCal applying the thresholds calculated from equation (2) for baselines below 10 counts or equation (1) when the baseline was higher than 10 counts. Regarding the total intensity of the particle events, less differences were observed for the three situations tested, with differences below 5% in any case.

In summary, the results obtained for counting particle events and determining their total intensity were in line with those expected considering the experimental uncertainty, and confirm that SPCal, under the selected conditions, processed the data conveniently for a variety of dwell times and baseline levels. Therefore, and taking into account that SPCal is an open source and free access tool, it can be used as a benchmark for the validation of other data processing tools to verify their reliability. Hence, the proprietary software Syngistix NanoModule v.3.2 from PerkinElmer was validated as a proof-of-concept following the same steps described above. Since there is no detailed information available about the workflow of this software, it was handled as a black-box, but using the critical values calculated from the approaches selected above, as in the case of using SPCal.

Regarding the processing of data with negligible baselines, as in the case of Au nanoparticle suspensions, Fig. 4a shows that data obtained for 30 nm Au nanoparticles with a dwell time of 50 μs and $Y_C = 6$ counts resulted in an underestimation of the counting events by Syngistix. For longer dwell times, the mean number of events obtained by Syngistix or

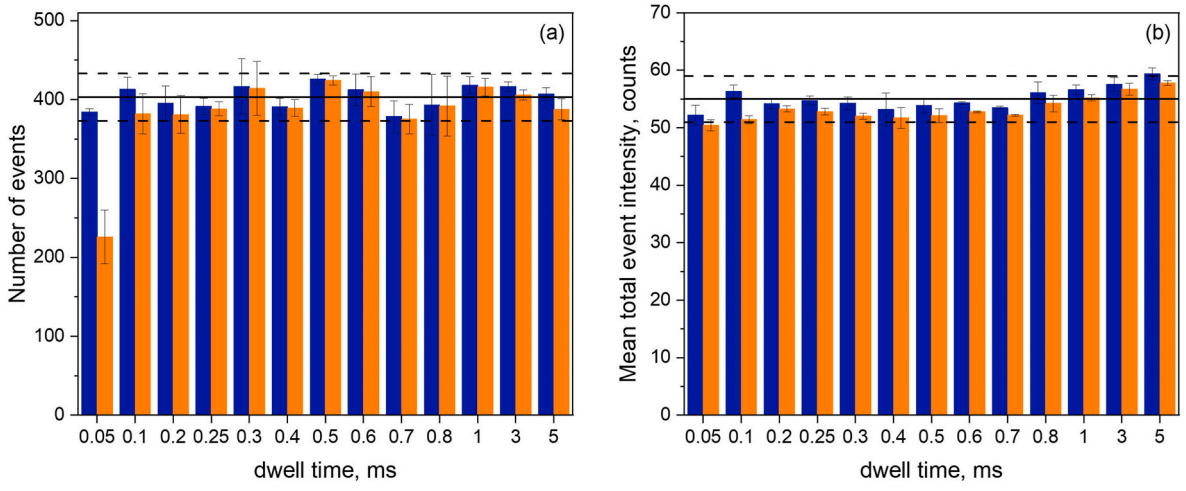


**Fig. 4.** (a) Number of particle events and (b) mean total intensity of particle events at different dwell times. Data processed with SPCal (blue) and Syngistix (orange) software. $Y_C = 6$ counts. 30 nm Au nanoparticle. Number concentration: $2.8x10^7$ $L^{-1}$. Line: Mean ± 2 x standard deviation (SPCal dataset). Bars: Mean ± standard deviation (n = 3).

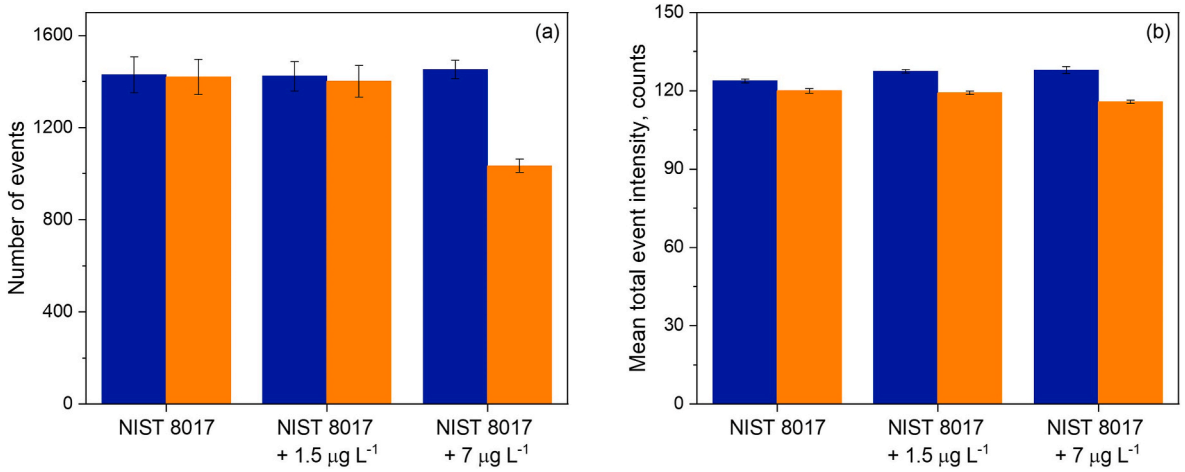


**Fig. 5.** (a) Number of particle events and (b) mean total intensity of particle events at different baseline levels (0.03, 2, 13 counts by addition of dissolved silver) measured in the analysis of 75 nm Ag nanoparticles (number concentration: 1 x $10^8$ $L^{-1}$). Data processed with SPCal (blue) and Syngistix (orange) software. Dwell time: 100 μs. Mean ± standard deviation (n = 3). Isotope monitored: $^{107}$Ag.

SPCal were not statistically different at the 95% confidence level, with mean number of events (± standard deviation) of 403 ± 15 and 397 ± 16 events for SPCal and Syngistix, respectively. Regarding the total intensity of particle events (Fig. 4b), the results obtained were not statistically different at the 95% confidence level, with mean total intensities (± standard deviation) of 55 ± 2 and 54 ± 1 counts for SPCal and Syngistix, respectively. The underestimation of the counting observed at 50 μs under the data processing conditions applied could be related to the small size of the particles (30 nm) and the short dwell time, in combination with the effect of the proprietary algorithms implemented in Syngistix, since this effect was not observed when measuring bigger Au nanoparticle suspensions (50 nm), as it can be seen in Fig SI4.

For higher baseline levels and bigger particles Fig. 5a confirms that the number of events did not show significant differences when processed with the Syngistix software for baseline intensities below 10 counts, whereas for baselines over 10 counts around 29 % of particle events were missed. Regarding the total intensity of the particle events, less differences were observed for the three situations tested, with differences below 5% in any case.

The effect of the baseline level was also studied with polystyrene microparticles, since relatively high baselines are expected when monitoring carbon isotopes due to the presence in the suspensions of carbon dioxide, surfactants or other carbon-containing species. In this case, a suspension of 3 μm polystyrene microparticles monitoring $^{13}$C showed a baseline intensity of 3.5 counts, whereas 14 counts were measured for a suspension of 2 μm polystyrene microparticles due to the higher surfactant content of the standard. Whereas for the 3 μm polystyrene suspension, equation (2) was used to calculate the threshold value, equation (1) had to be applied for the 2 μm suspension due to the higher baseline. Since no external references were available, the direct comparison of the results obtained from processing data with both tools was checked. As it can be seen in Fig. 6, SPCal processed microparticle events in a similar way than nanoparticles, despite showing broader intensity distributions both at low and high baseline intensities. For baseline intensities below 10 counts, both tools provided similar microparticle counts as well as mean total intensities, whereas for baselines above 10 counts, Syngistix underestimated the number of microparticles, although the total intensity remained comparable. Regarding the use of $^{12}$C for monitoring plastic microparticles, the increase on sensitivity of almost two orders of magnitude compared to $^{13}$C, due to their relative abundances, required handling baselines over 10 counts in any case and the application of equation (1) (Gauss filter) for calculation of critical values. As summarized in Figure SI5 and Table SI3, no significant differences were observed for counting and summing up

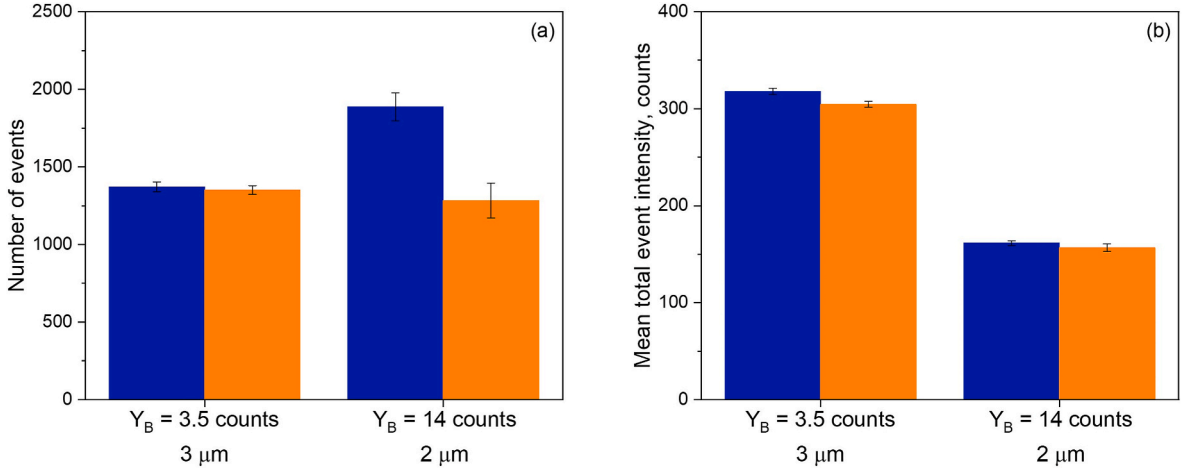


**Fig. 6.** (a) Number of particle events and (b) mean total intensity of particle events at different baseline levels (3.5, 14 counts) measured in the analysis of 3 and 2 μm polystyrene microparticles (number concentration: 3x$10^8$ $L^{-1}$). Data processed with SPCal (blue) and Syngistix (orange) software. Dwell time: 100 μs. Mean ± standard deviation (n = 3). Isotope monitored: $^{13}$C.

particle events when analyzing suspensions of 3 μm polystyrene microparticles.

From the results presented, it can be stated that Syngistix software behaved in a similar way than SPCal for counting and summing up particle events in the presence of baseline intensities below 10 counts when the same threshold values (calculated with equation (1) and/or 2) were applied, whereas for baselines over 10 counts, lower counting were observed both analyzing nanoparticle and microparticle suspensions, as shown in Figs. 5 and 6. Regarding the thresholds calculated by the Syngistix software (Table SI3), when its automatic 5-sigma option was selected, values different to those of SPCal were obtained since a Gaussian approach is always applied regardless the baseline intensity. However, for mean baselines below 0.1 counts, despite Syngistix applied a threshold of 1.01 counts, the number of particles detected were in agreement with those obtained by SPCal applying $Y_C = 6$ counts. In the case of $0.1 < Y_B < 10$ counts, both software also led to similar number of particles detected, despite the different thresholds applied. When facing higher baseline levels ($Y_B > 10$ counts) Syngistix software was not always able to handle data in a similar way to SPCal, underestimating the number of particles detected. Moreover, the 5-sigma threshold values provided by this software considerably varied from one replicate to another, which in the end affected the number of particles detected.

In summary, using the Syngistix software applying the 5-sigma threshold option allowed to obtain similar results to SPCal, except when the intensity of the particle events (in fact, their height) was not high enough with respect to the threshold applied (e.g., 75 nm Ag nanoparticles in the presence of 7 μg $L^{-1}$ Ag(I) or 2 μm PS microparticles, Table SI3; 30 nm Au nanoparticles at dwell times below 100 μs, Fig. 5a and SI.4.a). Since the proprietary software applies a different approach to calculating thresholds, but also includes other not known algorithms for data processing, the observed behavior cannot be clearly justified and it would be advisable to use this software with the manual threshold option instead of the automatic ones by entering the thresholds calculated from equations (1) and (2).

## 4. Conclusions

Although SP-ICP-MS can be considered a mature technique from an instrumental and methodological point of view, it still has serious limitations in terms of data processing due to the different approaches available and the lack of harmonization. This means that users cannot fully trust on current data processing tools to obtain reliable and accurate information. In this context, the availability of open-source and free-access data processing tools can contribute to consolidate the metrological harmonization that is required in this field.

Regarding the calculation of critical values for discrimination of readings corresponding to the baseline or to particle events, the application of equations (1) and (2) has proved to be adequate when handling intensities over or below 10 counts, respectively. In any case, coverage factors of $z_{1-\alpha} = 5$ ($\alpha \approx 10^{-7}$) must be selected to avoid the occurrence of false positives (readings from the baseline identified as particles) under a variety of data acquisition conditions. This is especially relevant since SP-ICP-MS datasets can contain more than 99% of baseline readings out of a total of millions-hundreds of thousands, depending on the dwell time and the total acquisition times selected. Although this approach has been checked for quadrupole instruments, equipped with electron multiplier detectors, it is also valid for double focusing instruments equipped with the same type of detectors. Application of less demanding criteria may lead to the misidentification of baseline readings as false particles that would degrade the detection capability in terms of number concentrations, whereas application of more restrictive criteria would affect the detectability of smaller particles or with lower element content. The suitability of the approach has been assessed with theoretical and experimental baselines but also in the presence of nano- and microparticles, confirming in the latter cases the occurrence of low intensity particle events that distort baselines when low-demanding criteria are applied. This effect was also observed when dwell times shorter than 100 μs were used, which would require the application of highly restrictive criteria if such short dwell times were to be used.

The software SPCal has proven to be highly accessible and flexible for applying critical value approaches, processing the resulting particle events in a reliable way, as confirmed by the results obtained, both for event counting and determination of their total intensities, in a variety of conditions (dwell times, baseline levels, analysis of nano- and microparticles). Consequently, SPCal can be considered a suitable reference for the validation of other data processing tools.

## CRediT authorship contribution statement

**Isabel Abad-Alvaro:** Writing – review & editing, Investigation, Data curation. **Eduardo Bolea:** Writing – review & editing, Supervision, Funding acquisition. **Francisco Laborda:** Writing – original draft, Supervision, Funding acquisition, Conceptualization.

## Declaration of competing interest

The authors declare that they have no known competing financial interests or personal relationships that could have appeared to influence the work reported in this paper.

## Acknowledgements

This work was funded by the Spanish Ministry of Science and Innovation (MCIN/AEI/10.13039/501100011033), project PID2021-123203OB-I00, "ERDF A way of making Europe" and the Government of Aragon, project E29_23R. I.A. thanks the European Union-Next Generation EU and the Spanish Ministry of Universities for funding under the María Zambrano Grant (MZ-240621). Authors would like to acknowledge the use of Servicio General de Apoyo a la Investigación-SAI, Universidad de Zaragoza.

## Appendix A. Supplementary data

Supplementary data to this article can be found online at https://doi.org/10.1016/j.talanta.2026.129575.

## Data availability

The data will be made available through Zenodo repository at https://doi.org/10.5281/zenodo.18745871

## References

[1] A. Hineman, C. Stephan, Effect of dwell time on single particle inductively coupled plasma mass spectrometry data acquisition quality, J. Anal. At. Spectrom. 29 (2014) 1252–1257, https://doi.org/10.1039/C4JA00097H.
[2] C. Degueldre, P.-Y. Favarger, Colloid analysis by single particle inductively coupled plasma-mass spectroscopy: a feasibility study, Colloids Surf. A Physicochem. Eng. Asp. 217 (2003) 137–142, https://doi.org/10.1016/S0927-7757(02)00568-X.
[3] E. Bolea, M.S. Jimenez, J. Perez-Arantegui, J.C. Vidal, M. Bakir, K. Ben-Jeddou, A. C. Gimenez-Ingalaturre, D. Ojeda, C. Trujillo, F. Laborda, Analytical applications of single particle inductively coupled plasma mass spectrometry: a comprehensive and critical review, Anal. Methods 13 (2021) 2742–2795, https://doi.org/10.1039/d1ay00761k.
[4] A. Laycock, N.J. Clark, R. Clough, R. Smith, R.D. Handy, Determination of metallic nanoparticles in biological samples by single particle ICP-MS: a systematic review from sample collection to analysis, Environ. Sci. Nano 9 (2022) 420–453, https://doi.org/10.1039/d1en00680k.
[5] K. Loeschner, M.E. Johnson, A.R. Montoro Bustos, Application of single particle ICP-MS for the determination of inorganic nanoparticles in food additives and food: a short review, Nanomaterials 13 (2023) 2547, https://doi.org/10.3390/nano13182547.
[6] G. Horlick, Inductively coupled plasma mass spectrometry: has it matured already? J Anal At Spectrom 9 (1994) 593–597, https://doi.org/10.1039/JA9940900593.
[7] P. Shaw, A. Donard, Nano-particle analysis using dwell times between 10 μs and 70 μs with an upper counting limit of greater than 3 × 10 7 cps and a gold nanoparticle detection limit of less than 10 nm diameter, J Anal At Spectrom 31 (2016) 1234–1242, https://doi.org/10.1039/C6JA00047A.

[8] R. Peters, Z. Herrera-Rivera, A. Undas, M. van der Lee, H. Marvin, H. Bouwmeester, S. Weigel, Single particle ICP-MS combined with a data evaluation tool as a routine technique for the analysis of nanoparticles in complex matrices, J Anal At Spectrom 30 (2015) 1274–1285, https://doi.org/10.1039/C4JA00357H.
[9] M.I. Chronakis, B. Meermann, M. von der Au, The evolution of data treatment tools in single-particle and single-cell ICP-MS analytics, Anal. Bioanal. Chem. 417 (2024) 7–13, https://doi.org/10.1007/s00216-024-05513-4.
[10] T.E. Lockwood, R. Gonzalez De Vega, D. Clases, An interactive Python-based data processing platform for single particle and single cell ICP-MS, J Anal At Spectrom 36 (2021) 2536–2544, https://doi.org/10.1039/d1ja00297j.
[11] T.E. Lockwood, L. Schlatt, D. Clases, SPCal – an open source, easy-to-use processing platform for ICP-TOFMS-based single event data, J Anal At Spectrom 40 (2025) 130–136, https://doi.org/10.1039/D4JA00241E.
[12] A. Gundlach-Graham, S. Harycki, S.E. Szakas, T.L. Taylor, H. Karkee, R. L. Buckman, S. Mukta, R. Hu, W. Lee, Introducing "time-of-flight single particle investigator" (TOF-SPI): a tool for quantitative spICP-TOFMS data analysis, J Anal At Spectrom 39 (2024) 704–711, https://doi.org/10.1039/D3JA00421J.
[13] ISO/TS 19590:2024, Nanotechnologies - Characterization of nano-objects Using Single Particle Inductively Coupled Plasma Mass Spectrometry, 2024.
[14] L.A. Currie, Limits for qualitative detection and quantitative determination: application to radiochemistry, Anal. Chem. 40 (1968) 586–593, https://doi.org/10.1021/ac60259a007.
[15] F. Laborda, J. Jiménez-Lamana, E. Bolea, J.R. Castillo, Critical considerations for the determination of nanoparticle number concentrations, size and number size distributions by single particle ICP-MS, J Anal At Spectrom 28 (2013), https://doi.org/10.1039/c3ja50100k.
[16] F. Laborda, A.C. Gimenez-Ingalaturre, E. Bolea, J.R. Castillo, About detectability and limits of detection in single particle inductively coupled plasma mass spectrometry, Spectrochim. Acta Part B At. Spectrosc. 169 (2020) 105883, https://doi.org/10.1016/j.sab.2020.105883.
[17] H.E. Pace, N.J. Rogers, C. Jarolimek, V. a Coleman, C.P. Higgins, J.F. Ranville, Determining transport efficiency for the purpose of counting and sizing nanoparticles via single particle inductively coupled plasma mass spectrometry, Anal. Chem. 83 (2011) 9361–9369, https://doi.org/10.1021/ac201952t.
[18] L. Hendriks, A. Gundlach-Graham, D. Günther, Performance of sp-ICP-TOFMS with signal distributions fitted to a compound poisson model, J Anal At Spectrom 34 (2019) 1900–1909, https://doi.org/10.1039/C9JA00186G.
[19] A. Ulianov, O. Müntener, U. Schaltegger, The ICPMS signal as a poisson process: a review of basic concepts, J Anal At Spectrom 30 (2015) 1297–1321, https://doi.org/10.1039/c4ja00319e.
[20] A. Gundlach-Graham, L. Hendriks, K. Mehrabi, D. Günther, Monte Carlo simulation of low-count signals in time-of-flight mass spectrometry and its application to single-particle detection, Anal. Chem. 90 (2018) 11847–11855, https://doi.org/10.1021/acs.analchem.8b01551.
[21] F. Laborda, A.C. Gimenez-Ingalaturre, E. Bolea, J.R. Castillo, Single particle inductively coupled plasma mass spectrometry as screening tool for detection of particles, Spectrochim. Acta Part B At. Spectrosc. 159 (2019) 105654, https://doi.org/10.1016/j.sab.2019.105654.
[22] A. Gundlach-Graham, R. Lancaster, Mass-dependent critical value expressions for particle finding in single-particle ICP-TOFMS, Anal. Chem. 95 (2023) 5618–5626, https://doi.org/10.1021/acs.analchem.2c05243.
[23] J. Tuoriniemi, G. Cornelis, M. Hassellöv, Size discrimination and detection capabilities of single-particle ICPMS for environmental analysis of silver nanoparticles, Anal. Chem. 84 (2012) 3965–3972, https://doi.org/10.1021/ac203005r.
[24] T. Lockwood, SPCal v 1.3.3. https://github.com/djdt/spcal/releases/tag/v1.3.3, 2025.
[25] L.A. Currie, On the detection of rare, and moderately rare, nuclear events, J. Radioanal. Nucl. Chem. 276 (2008) 285–297, https://doi.org/10.1007/s10967-008-0501-5.
[26] MARLAP, 20 Detection and Quantification, in: Multi-Agency Radiological Laboratory Analytical Protocols Manual, 2004.
[27] K. Mehrabi, R. Kaegi, D. Günther, A. Gundlach-Graham, Emerging investigator series: automated single-nanoparticle quantification and classification: a holistic study of particles into and out of wastewater treatment plants in Switzerland, Environ. Sci. Nano 8 (2021) 1211–1225, https://doi.org/10.1039/d0en01066a.
[28] S.G. Bevers, C. Smith, S. Brown, N. Malone, D.H. Fairbrother, A.J. Goodman, J. F. Ranville, Improved methodology for the analysis of polydisperse engineered and natural colloids by single particle inductively coupled plasma mass spectrometry (spICP-MS), Environ. Sci. Nano 10 (2023) 3136–3148, https://doi.org/10.1039/d3en00425b.
[29] A.C. Gimenez-Ingalaturre, K. Ben-Jeddou, J. Perez-Arantegui, M.S. Jimenez, E. Bolea, F. Laborda, How to trust size distributions obtained by single particle inductively coupled plasma mass spectrometry analysis, Anal. Bioanal. Chem. 415 (2023) 2101–2112, https://doi.org/10.1007/s00216-022-04215-z.
[30] J. Liu, K.E. Murphy, R.I. MacCuspie, M.R. Winchester, Capabilities of single particle inductively coupled plasma mass spectrometry for the size measurement of nanoparticles: a case study on gold nanoparticles, Anal. Chem. 86 (2014) 3405–3414, https://doi.org/10.1021/ac403775a.
[31] D. Mozhayeva, C. Engelhard, A quantitative nanoparticle extraction method for microsecond time resolved single-particle ICP-MS data in the presence of a high background, J Anal At Spectrom 34 (2019) 1571–1580, https://doi.org/10.1039/c9ja00042a.
[32] I. Kálomista, A. Kéri, D. Ungor, E. Csapó, I. Dékány, T. Prohaska, G. Galbács, Dimensional characterization of gold nanorods by combining millisecond and microsecond temporal resolution single particle ICP-MS measurements, J Anal At Spectrom 32 (2017) 2455–2462, https://doi.org/10.1039/c7ja00306d.
[33] A. Bazo, E. Bolea-Fernandez, A. Rua-Ibarz, M. Aramendía, M. Resano, Intensity- and time-based strategies for micro/nano-sizing via single-particle ICP-mass spectrometry: a comparative assessment using Au and SiO2 as model particles, Anal. Chim. Acta 1331 (2024) 343305, https://doi.org/10.1016/j.aca.2024.343305.